Mechanisms of Photocatalytical Degradation of Monomethylarsonic and Dimethylarsinic Acids Using Nanocrystalline Titanium Dioxide

ARTICLE *in* ENVIRONMENTAL SCIENCE AND TECHNOLOGY · APRIL 2008

Impact Factor: 5.33 · DOI: 10.1021/es0719677 · Source: PubMed

4 AUTHORS, INCLUDING:

Zhonghou Xu
Stevens Institute of Technology
13 PUBLICATIONS **237** CITATIONS
SEE PROFILE

Chuanyong Jing
Research Center for Eco-Environmental Sci…
70 PUBLICATIONS **1,255** CITATIONS
SEE PROFILE

Xiaoguang Meng
Stevens Institute of Technology
83 PUBLICATIONS **3,552** CITATIONS
SEE PROFILE

Mechanisms of Photocatalytical Degradation of Monomethylarsonic and Dimethylarsinic Acids Using Nanocrystalline Titanium Dioxide

ZHONGHOU XU,[†] CHUANYONG JING,[†,§] FASHENG LI,[‡] AND XIAOGUANG MENG*[,†]

Center for Environmental Systems, Stevens Institute of Technology, Hoboken, New Jersey 07030, and Laboratory of Soil Pollution Control, Chinese Research Academy of Environmental Sciences, Beijing 100012, China

Received August 7, 2007. Revised manuscript received November 23, 2007. Accepted January 5, 2008.

Photodegradation mechanisms of monomethylarsonic acid (MMA) and dimethylarsinic acid (DMA) with nanocrystalline titanium dioxide under UV irradiation were investigated. In the presence of UV irradiation and 0.02 g/L TiO_2, 93% MMA (initial concentration is 10 mg-As/L) was transformed into inorganic arsenate, [As(V)], after 72 h of a batch reaction. The mineralization of DMA to As(V) occurred in two steps with MMA as an intermediate product. The photodegradation rate of MMA and DMA could be described using first-order kinetics, where the apparent rate constant is 0.033/h and 0.013/h for MMA and DMA, respectively. Radical scavengers, including superoxide dimutase (SOD), sodium bicarbonate, tert-butanol, and sodium azide, were used to study the photodegradation mechanisms of MMA and DMA. The results showed that hydroxyl radicals ($HO^{\bullet}$) was the primary reactive oxygen species for the photodegradation of MMA and DMA. The methyl groups in MMA and DMA were transformed into organic carbon, including formic acid and possibly methanol, also through photochemical reactions. The results showed that nanocrystalline TiO_2 can be used for the photocatalytical degradation of MMA and DMA and subsequent removal of the converted As(V), since the high adsorption capacity of the material for inorganic arsenic species has been demonstrated in previous studies.

Introduction

Arsenic is a naturally occurring and ubiquitous element found in terrestrial as well as aquatic environments. Inorganic arsenate As(V) and arsenite As(III), organic monomethylarsonic acid (MMA), and dimethylarsinic acid (DMA) are four commonly found arsenic species in the environment. Despite the fact that inorganic arsenic species are predominant, the presence of MMA and DMA in natural waters has also been reported (*1–3*). In addition to the methylation of As(V) carried out by a variety of organisms ranging from bacteria to fungi to mammals (*4*), anthropogenic input of organic arsenic compounds arose since the 1970s due to their increasing usage as pesticides and herbicides worldwide (*5*). Organic arsenicals such as MMA and DMA are considered to be less toxic than inorganic arsenic species (*6*), and are still used as herbicides on agricultural lands, orchards, and golf courses. U.S. statistics indicate that between 2 and 4 million pounds of the sodium salt of MMA (monosodium methylarsonate, MSMA) was used in the U.S. during 1999 by industrial, commercial, and government sectors (*7*). In Florida, end-use registrants sold an equivalent of 403 000 pounds of the MSMA active ingredient, equivalent to 85 t of arsenic, during 2002 (*5*).

High concentrations of organic arsenic have been detected in groundwater samples. According to Del Razo et al. (*8*), a high DMA concentration of 20 μg/L was observed in well water samples collected from northern Mexico. DMA has been detected in most of the groundwater samples in northeast and northwest Taiwan (*9*). Anderson and Bruland (*1*) reported that methylated arsenic species, predominantly DMA, were on an average of 24% of the total dissolved As in the lakes surveyed in California. Groundwater at a superfund site in the northeastern U.S. had organic arsenic concentrations as high as 30 mg/L, which represents about 10% of the total arsenic (*3*).

Compared to a large body of literature on removal of inorganic arsenic from water, only a few studies have been conducted to investigate the treatment of organic arsenic in water (*10–12*). Previous studies focus on adsorption of MMA and DMA using different materials including activated carbon, manganese greensand, iron oxide-coated sand, and resin (*10–12*). The removal of MMA and DMA by these adsorbents is less efficient than that of inorganic arsenic species (*12*). Recently, a nanocrystalline-based anatase TiO_2 adsorbent has been developed for effective removal of As(V) and As(III) (*13*). The material has a moderate and low adsorption capacity for MMA and DMA, respectively (*14*). If the organic arsenic species can be effectively transformed into As(V), the inorganic arsenic species can be easily removed by the adsorbent or with coprecipitation treatment. The photochemical degradation of organoarsenic compounds has been studied to develop an analytical procedure (*15*). Nakajima et al. (*16*) used a combination of TiO_2-photocatalyst and adsorbents, such as activated alumina and carbon, to remove As(III), MMA, and DMA from aqueous media under photoirradiation. Xu et al. (*17*) studied adsorption and photocatalyzed oxidation of MMA and DMA in TiO_2 (Degussa P25) suspensions. The results have demonstrated that TiO_2 can be used for the photodegradation of MMA and DMA to As(V). However, the mechanisms of MMA and DMA photodegradation and especially the reaction products of the methyl groups are not well understood.

Major photoreactions in the TiO_2 system are summarized in Table S1 in the Supporting Information (*18–21*). TiO_2 is a semiconductor, and adsorption of a photon with enough energy leads to a charge separation due to an electron promotion to the conduction band and a generation of a hole (h^+) in the valence band. These charge carriers may migrate to the particle surface where they are trapped. Usually, electron transfer to dissolved oxygen, which acts as primary electron acceptor, is the rate-determining step in photocatalysis (*20*). The photogenerated electrons react with adsorbed oxygen to produce superoxide ($O_2^{\bullet -}$). This superoxide is an effective oxygenation agent that attacks neutral substrates as well as surface-adsorbed radicals and radical ions. Hydroxyl radicals are formed through reactions of $O_2^{\bullet -}$ and h^+ with adsorbed H_2O, hydroxide, surface titanol groups (>TiOH), and other species. Theoretically, the redox potential

* Corresponding author phone: +1 201 2168014; fax: +1 201 2188303; e-mail: xmeng@stevens.edu.
[†] Stevens Institute of Technology.
[‡] Chinese Research Academy of Environmental Sciences.
[§] Current address: Research Center for Eco-Environmental Sciences, Chinese Academy of Sciences, Beijing 100085, China.

10.1021/es0719677 CCC: $40.75
Published on Web 02/26/2008

of the electron–hole pair permits H_2O_2 formation. The main pathway of H_2O_2 formation is by two conduction band electron reduction of the adsorbed oxygen (*22, 23*). H_2O_2 contributes to the degradation pathway by acting as an electron acceptor or as a direct source of hydroxyl radicals due to homolytic scission (*20*). Recently, the formation of singlet oxygen ($^1O_2$) in TiO_2 photocatalysis was directly detected (*24*). Holes, $HO^{\bullet}$, $O_2^{\bullet-}$, H_2O_2, or $^1O_2$ can play important roles in the photocatalytical reactions under different conditions.

This study is focused on the understanding of photocatalytical degradation mechanisms of MMA and DMA in the presence of nanocrystalline TiO_2 and UV irradiation. Four radical scavengers were used to delineate the major radicals responsible for the degradation of MMA and DMA. The demethylation pathways were investigated by analyzing the reaction products of methyl groups.

Materials and Methods

Materials. Nanocrystalline TiO_2 in anatase form was prepared by hydrolysis of a titanium sulfate solution (*25*). The primary crystalline size and BET surface area of the particles were about 6 nm and 330 m^2/g, respectively (*13, 14*). The material has been used as an adsorbent in household and industrial filters for the treatment of arsenic, lead, and other heavy metals in water. Dimethylarsinic acid (DMA, $C_2H_7AsO_2$) was purchased from Sigma Chemical in Minnesota. Monosodium acid methane arsonate sesquihydrate (MMA, $CH_4AsNaO_3 \cdot 1.5\ H_2O$) was purchased from Chem Service in Pennsylvania. Sodium bicarbonate ($NaHCO_3$), sodium azide (NaN_3) and tert-butanol were certified A.C.S grade and purchased from Fisher Scientific Inc. Superoxide dimutase (SOD, activity: 3500 units/mg, molecular weight: ~32 500 Daltons) was also purchased from Fisher Scientific Inc.

Photodegradation Experiments. Photocatalytic degradation of MMA and DMA was tested in batch experiments. A 1 L solution containing 0.04 M NaCl, 0.020 mg/L of TiO_2, initial MMA or DMA concentration of 10 mg-As/L, and at circum-neutral pH was prepared at the beginning of each experiment. The solution in a 1 L glass beaker was covered with aluminum foil and was mixed with a magnetic stirrer for 24 h to disperse large TiO_2 aggregates and to reach adsorption equilibrium of MMA and DMA on TiO_2. Then, the solution was illuminated with UV light (wavelength 254 nm) using a 150 V bench ultra violet lamp (model XX-15S, UVP LLC, CA) which was placed 15 cm above the solution. At desired reaction times, uniform suspension samples were withdrawn from the beaker. The samples were centrifuged immediately at 10 000 rpm for 10 min for analysis of soluble MMA, DMA, and their degradation products using high-performance liquid chromatography coupled with an atomic fluorescence system (HPLC-AFS, PS Analytical Millennium). The detailed procedure for the analysis was described by Gomez-Ariza et al. (*26*). To study the reaction products of methyl groups in the organoarsenics, the total organic carbon (TOC) and total carbon (TC) concentrations in solution was analyzed using a TOC Analyzer with UV-persulfate (Phoenix 8000). Formic acid (HCOOH) was determined using ion chromatography (IC25, DIONEX) with an AS16 column (4 × 250 mm).

In another set of batch experiments, scavengers including $NaHCO_3$ (100 and 200 mg/L HCO_3^-), tert-butanol (50 and 100 mg/L), NaN_3 (100 mg/L N_3^-), a combination of NaN_3 and $NaHCO_3$ (100 mg/L N_3^- and 200 mg/L HCO_3^-), and SOD (2000 and 4000 units/mL), were added into the solution to determine the effect of different radicals on the photocatalytical degradation. For all the above experiments, the position of the reactors was carefully controlled to be at the same place and to eliminate differences in UV light intensity between experiments. In general, duplicate experiments were conducted for each system, and the experimental error was about ± 5%.

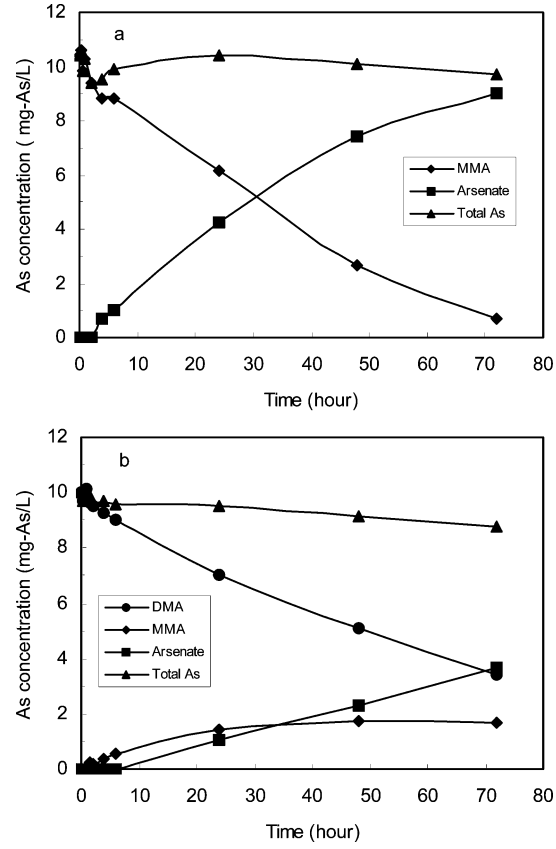

FIGURE 1. Photodegradation processes of MMA (a) and DMA (b). Initial MMA= DMA = 10 mg-As/L, TiO_2 = 0.02 g/L, ionic strength = 0.04 M NaCl.

During the experiments, the pH was not controlled and it decreased from 7 to about 5 in the solutions without the radical scavengers. Xu et al. (*17*) reported that pH had little effect on photodegradation rate of MMA and DMA in a pH rang between 3 and 7. In the systems containing the scavengers, the pH decreased by less than 0.5 pH unit.

Results and Discussion

Photodegradation of MMA and DMA. The photodegradation processes of MMA and DMA are illustrated in Figure 1. MMA was reduced from an initial concentration of 10−0.7 mg-As/L during 72 h of reaction (Figure 1a). Meanwhile, the As(V) concentration increased from 0 to 9.0 mg/L. The sum of MMA and As(V) concentrations at different reaction times was approximately the same as the initial MMA concentration of 10 mg-As/L, which indicated that all degraded MMA molecules were converted to As(V) species. The results also suggested that very little arsenic species were adsorbed by TiO_2, due to the high As/TiO_2 ratio (10 mg/0.02 g) used in the suspension. The control experimental results in Supporting Information Figure S1 show that there was no decrease in MMA and DMA concentrations in the presence of TiO_2 without UV irradiation. The fact that MMA and DMA concentrations remained near 10 mg/L during 72 h of mixing in other control systems containing no TiO_2 and with UV irradiation (Figure S1) demonstrated that UV light alone will not cause degradation of MMA and DMA. The results were consistent with those reported in the literature (*17*).

During the degradation of DMA, both MMA and As(V) were formed in the solution (Figure 1b). DMA was first transformed into MMA by losing a methyl group, and then was degraded to As(V). The DMA concentration was reduced

TABLE 1. First-Order Kinetic Constants of MMA and DMA

	MMA		DMA	
treatment systems	k (10^{-2} hr^{-1})	R^2	k (10^{-2} hr^{-1})	R^2
control (no scavenger)	3.3	0.969	1.3	0.998
HCO_3^-, 100 mg/L	0.71	0.993	0.22	0.992
HCO_3^-, 200 mg/L	0.51	0.935	0.15	0.980
tert-C_4H_9OH, 50 mg/L	1.4	0.997	0.98	0.997
tert-C_4H_9OH, 100 mg/L	1.2	0.990	0.82	0.998
N_3^-, 100 mg/L	0.63	0.999	1.3	0.990
N_3^-, 100 mg/L and HCO_3^-, 200 mg/L	0.34	0.950	0.06	0.901
SOD, 2000 units/mL	0.09	0.917	0.01	0.934
SOD, 4000 units/mL	0.08	0.906	NA[a]	NA[a]

[a] The photodegradation of DMA was completely inhibited.

gradually from 10 to 3.5 mg-As/L after 72 h. MMA, an intermediate of the DMA photodegradation process, increased from zero to 1.8 mg-As/L in the first 48 h and remained at a steady state level thereafter. The As(V) concentration increased almost linearly with the increase of UV-irradiation time. The sum of MMA, As(V), and DMA concentrations in the solution at any reaction time was almost equal to the initial DMA concentration of 10 mg-As/L. The above MMA and DMA photodegradation process agreed with the results reported by Nakajima et al. (*16*), Sun et al. (*27*) and Xu et al. (*17*). Complete demethylation of MMA and DMA to As(V) within 60 min was observed by Xu et al. (*17*) because a high As/TiO_2 ratio (1 mg/0.1 g) was used in their experiments.

Linear regression analysis was performed to fit the MMA and DMA photodegradation data in Figure 1 to the first order kinetic equation (*28*). The rate constant k was obtained as 3.3×10^{-2} hr^{-1} ($R^2 = 0.969$) and 1.3×10^{-2} hr^{-1} ($R^2 = 0.998$) for MMA and DMA, respectively (Table 1). The high R^2 values indicated that the photodegradation of MMA and DMA could be described well with the first order expression.

Contribution of Different Radicals to Photodegradation of MMA and DMA. In the presence of UV irradiation and TiO_2, various reactive oxygen species, including $HO^\bullet$, $O_2^{\bullet-}$, H_2O_2, and $^1O_2$, are generated (*20*). It has been reported that $HO^\bullet$ plays an important role in the photodegradation of MMA and DMA (*16, 17*). The contribution of the other radicals to the photodegradation of MMA and DMA has not been investigated. We utilized four selective radical scavengers to assess the extent of MMA and DMA degradation caused by $O_2^{\bullet-}$, $HO^\bullet$, and $^1O_2$ in this study. The scavengers and their reactions with free radicals are summarized in Supporting Information Table S2. SOD catalyzes the dismutation of superoxide radical to hydrogen peroxide and molecular oxygen with a rate constant of 2×10^9 M^{-1} s^{-1} (Table S2). It can also react with other free radicals and as a result of the reactions it is inactivated (*29–31*). Bicarbonate and tert-butanol selectively quench hydroxyl radical. Azide reacts with both singlet oxygen and hydroxyl radical.

The inhibition effect of scavengers on MMA photodegradation is shown in Figure 2. Among the scavengers tested, SOD had the most dramatic effect on MMA degradation. When the SOD concentration was 2000 units/mL, it almost completely inhibited the photodegradation of MMA (Figure 2a). After 72 h of reaction the MMA concentration decreased slightly, from 10 to 9.3 mg-As/L, in stark contrast to the final concentration of 0.7 mg-As/L in the control system (without scavenger). Meanwhile, only 0.7 mg/L As(V) was formed in the presence of SOD (Figure 2b). The first order rate constant k decreased from 3.3×10^{-2} hr^{-1} for the control system to 9.0×10^{-4} and 8.0×10^{-4} hr^{-1} for SOD concentrations of 2000 and 4000 units/mL, respectively (Table 1). The lines in

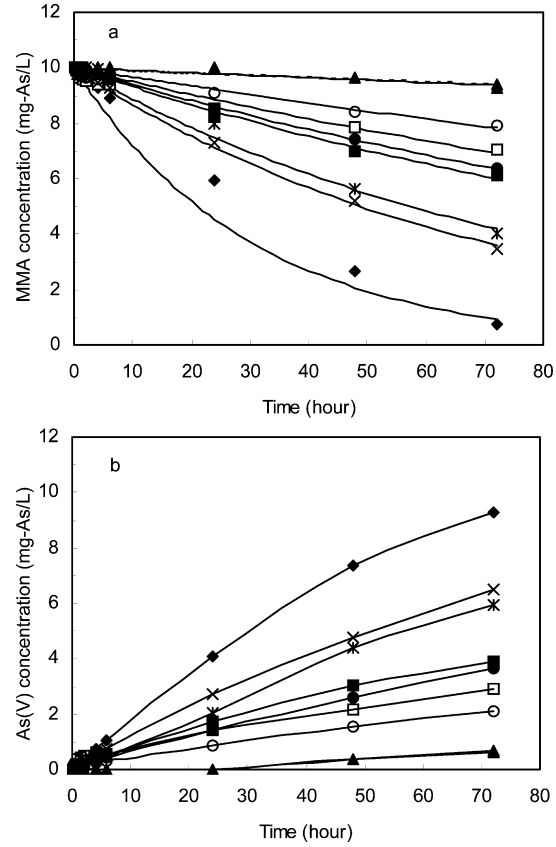

FIGURE 2. Effect of scavengers on photodegradation of MMA and the best fitting lines calculated with first order kinetic model (a) and formation of As(V) (b). Initial MMA= DMA = 10 mg-As/L, TiO_2 = 0.02 g/L, ionic strength = 0.04 M NaCl. Bicarbonate 100 (■) and 200 (□) mg/L, *t*-butanol 50 (×), and 100 (*) mg/L, azide (●), azide and bicarbonate (○), SOD 2 (▲) and 4 (Δ) ku/mL, and control system (♦).

Figure 1a were calculated with the first order kinetic equation and best-fit constants in Table 1. The results suggest $O_2^{\bullet-}$ and $HO^\bullet$ played a predominant role in MMA photodegradation. Superoxide was dismutated by SOD into H_2O_2 and O_2, which are less reactive than superoxide radical.

Bicarbonate is a well-known $HO^\bullet$ scavenger and is present in surface and ground waters at concentrations typically in a range of 50–200 mg/L (*32*). The presence of bicarbonate significantly decreased the rate of MMA degradation (Figure 2a, Table 1). When bicarbonate was 100 and 200 mg/L and after 72 h of reaction, the MMA concentration was decreased from 10 to 6.1 and 7.1 mg/L, respectively. The first order rate constant was decreased from 3.3×10^{-2} hr^{-1} for the control system to 7.1×10^{-3} and 5.1×10^{-3} hr^{-1} for the 100 and 200 mg/L of bicarbonate systems, respectively (Table 1). Higher concentrations of bicarbonate caused greater reductions in the rate of MMA degradation. However, even at the relatively high bicarbonate concentration of 200 mg/L, there was still 29% MMA degradation that might be attributed to the existence of superoxide. The results suggested that $HO^\bullet$ was an important radical for MMA degradation.

Another commonly used $HO^\bullet$scavenger is tert-butanol, which caused a moderate inhibition of the degradation rate of MMA (Figure 2a). When the tert-butanol concentration increased from 50 to 100 mg/L, the inhibition effect increased slightly. The inhibition effect of tert-butanol on the photocatalytical oxidation of MMA and DMA was also reported by Xu et al. (*17*).

Azide, a scavenger for $HO^\bullet$and $^1O_2$, also significant reduced the degradation rate of MMA (Figure 2a). In order to assess

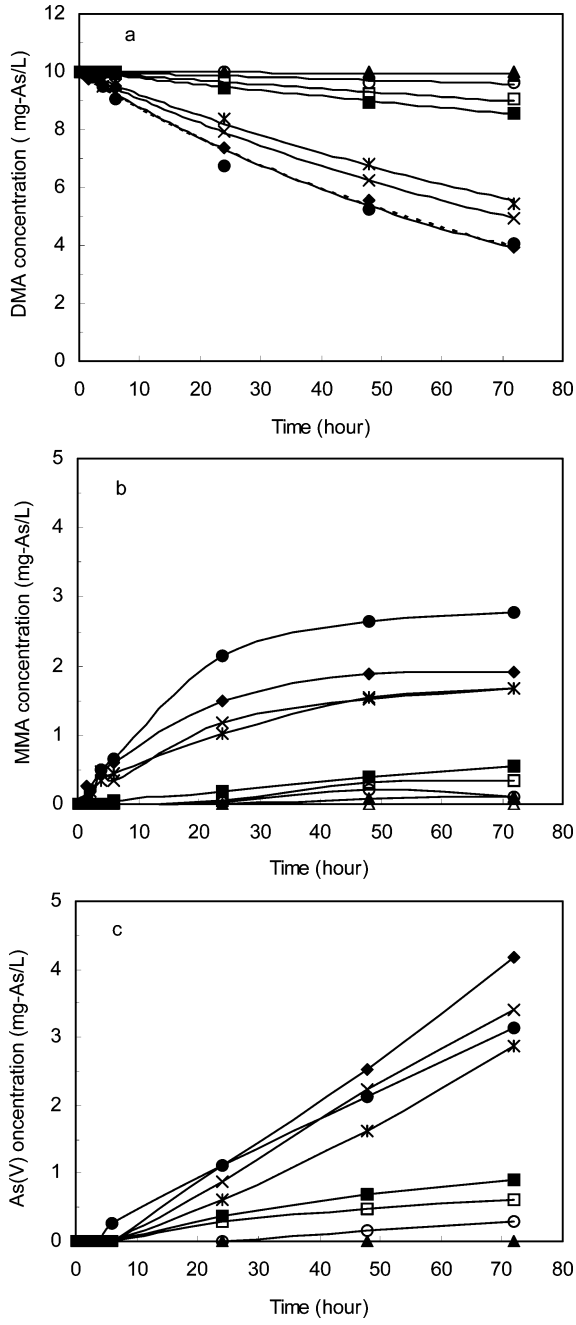

FIGURE 3. Effect of scavengers on photodegradation of DMA and best fitting lines calculated with first order kinetic model (a), concentration profile of MMA (b), and formation As(V) (c). Initial MMA= DMA = 10 mg-As/L, TiO_2 = 0.02 g/L, ionic strength = 0.04 M NaCl. Bicarbonate 100 (□) and 200 (■) mg/L, *t*-butanol 50 (×) and 100 (*) mg/L, azide (●), azide with bicarbonate (○), SOD 2 (▲) and 4 (Δ) ku/mL, and control system (♦).

the contribution of $^1O_2$ to the degradation, a combination of 100 mg/L azide and 200 mg/L of bicarbonate was used in a test. The inhibition effect of the combined scavengers was slightly greater than 200 mg/L bicarbonate, which suggests that $^1O_2$ might cause a small amount of MMA degradation.

The four radical scavengers, except azide, had similar inhibition effects on DMA photodegradation (Figure 3) to those on MMA. The hindering extent of SOD, bicarbonate, and tert-butanol was near complete, significant, and moderate, respectively. Azide had no effect on DMA degradation (Figure 3a), compared to its significant effect on MMA

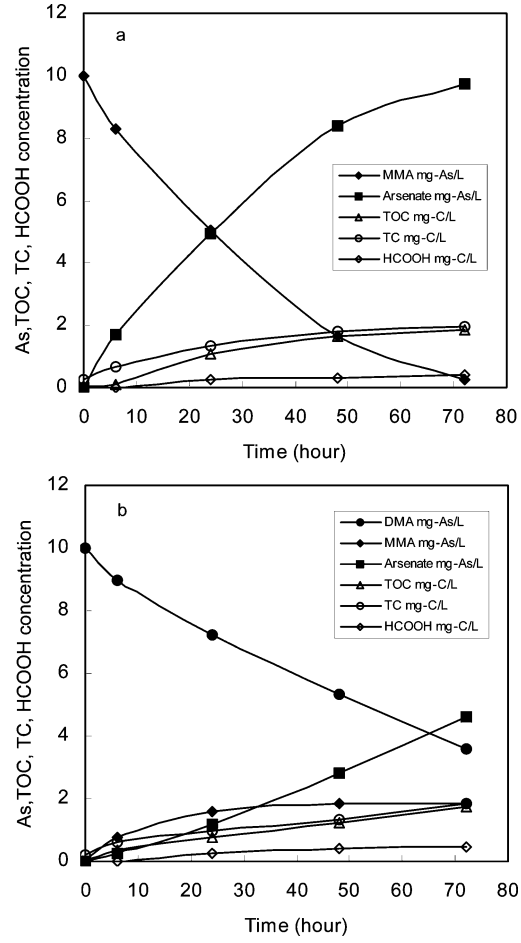

FIGURE 4. Variation of TOC, TC, and HCOOH concentrations during the photodegradation process of MMA (a) and DMA (b). Initial MMA = DMA = 10 mg-As/L, TiO_2 = 0.02 g/L, ionic strength = 0.04 M NaCl.

degradation (Figure 2a). The results indicated that the degradation of DMA was also mainly caused by $HO^•$ and $O_2^{•-}$.

Since the first step demethylation of DMA was not inhibited, and the demethylation of MMA was significantly hindered by azide, the MMA concentration accumulated in the solution to higher levels (up to 2.8 mg-As/L) than in the control system (Figure 3b). On the other hand, the MMA concentration remained very low (less than 0.6 mg-As/L) in the bicarbonate system because bicarbonate has more effect on degradation of DMA than for MMA. The higher As(V) concentration compared to MMA in the carbonate systems (Figure 3c) also showed that the degradation of MMA was not the rate limiting reaction for mineralization of DMA to As(V).

Demethylation Process of MMA and DMA. Under the attack of $HO^•$ and $O_2^{•-}$, DMA and MMA were demethylated to form As(V). However, the demethylation pathways and fate of methyl groups have not been fully established in previous studies (*16, 17, 27*). In order to improve the understanding of these reactions, TOC, TC, and HCOOH concentrations were monitored during the photodegradation tests, and the results are presented in Figure 4. Before the TiO_2 suspension containing 10 mg-As/L of MMA or DMA was irradiated with UV light, TOC in the centrifuged solution was less than 0.1 mg-C/L. According to the chemical formula of MMA ($CH_3AsNa_2O_3H$) and DMA ($CH_3CH_3AsO_2H$), the carbon to arsenic mass ratio (C/As) in the two compounds is 0.16 and 0.32, respectively. If the carbon in 10 mg-As/L of MMA solution is completely converted to organic carbon, a

TABLE 2. Mass Balance of Carbon in MMA and DMA Solutions before and after Photodegradation

	total C in 10 mg-As/L org-As (mg-C/L)	C (mg-C/L) in different forms after 72 h reaction					
		DMA	MMA	TC	TOC	HCOOH	other org-C
MMA $CH_3AsNa_2O_3H$	1.6	NA	0.1	2.0−0.3	1.8	0.4	1.8 − 0.4 = 1.4
DMA $CH_3CH_3AsO_2H$	3.2	1.2	0.3	1.8	1.8	0.4	1.8 − 0.4 = 1.4

TOC of 1.6 mg-C/L should be measured in the TOC analysis. The result indicated that no MMA and DMA could be oxidized to CO_2 with UV-persulfate in the TOC analysis.

When the suspension containing MMA was under UV irradiation for 72 h, the MMA concentration decreased from 10 to 0.3 mg-As/L, and TOC increased to about 1.8 mg-C/L (Figure 4a, Table 2). The results indicated that all carbon in MMA was converted to organic carbon forms that could be detected in the TOC analysis. The slightly higher than theoretical TOC values measured can be attributed to analytical errors. During 72 h of UV irradiation, TC increased from 0.3 mg-C/L in the initial suspension to 2.0 mg-C/L. The small amount of TC in the initial suspension could be caused by dissolved CO_2. The TC and TOC concentrations remained similar during the experiment, which also suggested that no inorganic carbon, such as CO_2, was formed in the demethylation process of MMA.

During the degradation process, formic acid was formed and its concentration increased from 0 to 0.4 mg-C/L (Figure 4a, Table 2). The difference between the concentrations of TOC and formic acid implied that about 1.4 mg-C/L of other organic byproducts were formed during the photodegradation of MMA. Methyl groups could be oxidized to methanol and formaldehyde. The photochemical oxidation of methanol is slow (reaction 1 in Table S3), whereas formaldehyde can be readily oxidized to formic acid according to reaction 4 in Table S3. Therefore, methanol is another possible organic compound in the system.

The transformation of DMA methyl groups was similar to that of MMA (Figure 4b). The total carbon content in a suspension containing 10 mg-As/L of DMA was 3.2 mg-C/L. When the suspension was irradiated for 72 h, the DMA concentration decreased to 3.6 mg-As/L (containing 1.2 mg-C/L) and the MMA concentration increased to 1.8 mg-As/L (containing 0.3 mg-C/L) (Table 2). Based on the mass balance of carbon in the initial DMA and in the residual DMA and MMA, 1.7 mg/L of carbon was released from DMA. Analytical results showed that TOC and TC concentrations increased to about 1.8 mg-C/L. The formic acid concentration increased to about 0.4 mg-C/L. The results indicated that all demethylated methyl groups were converted to organic compounds including about 0.4 mg-C/L of formic acid.

Photodegradation Pathways of MMA and DMA. Based on the findings discussed above and the literature information on free radical chemistry, three photodegradation reactions are proposed (reactions 1–3, where R = OH or CH_3). Free hydroxyl radical may react with MMA and DMA in two pathways as described in reactions 1 and 2. $HO^\bullet$ is a strongly oxidizing species, which can promote a variety of reactions. In spite of its high oxidizing power, $HO^\bullet$ reacts preferentially by addition to electron-rich aromatic and olefinic moieties rather than by outer sphere electron transfer (*33, 34*). To a lesser extent, $HO^\bullet$ can extract hydrogen atoms from saturated carbon atoms. Therefore, hydroxyl radical may attack the double bond between arsenic and oxygen (reaction 1) or the methyl groups (reaction 2) of DMA and MMA. In reaction 1, a one step demethylation process occurs to produce As(V) and $CH_3^\bullet$, which is analogous to the TiO_2-mediated photodegradation of dimethyl methylphosphonate (*35, 36*). In the second pathway, an alkyl radical is formed due to a hydrogen extraction reaction by the hydroxyl radical, which is similar to the hydrogen extraction reactions of diuron and dimethyl methylphosphonate (*35, 37*). Under successive attack of $HO^\bullet$, DMA was transformed into MMA which was further attacked by $HO^\bullet$ and mineralized to As(V).

Superoxide radicals exist in an acid–base equilibrium with $pK_a = 4.8$ (*20*). They may attack the double bonds between arsenic and oxygen atoms in DMA and MMA (reaction 3). An unstable intermediate is formed and rapidly degrades into As(V) and $CH_3O^\bullet$.

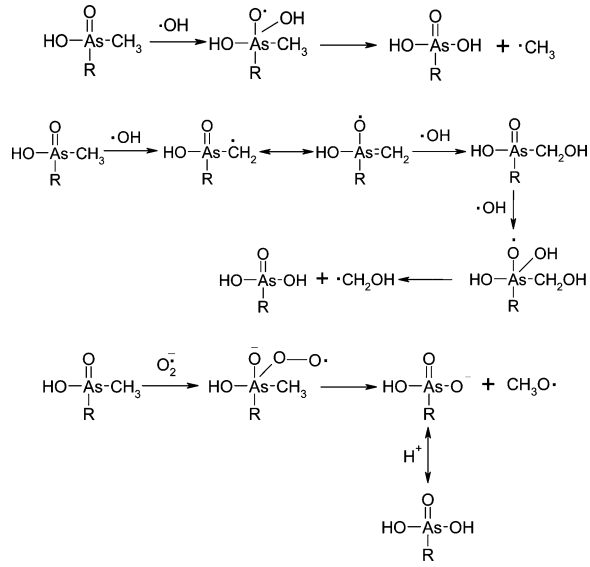

The $^\bullet CH_3$, $^\bullet CH_2OH$, and $CH_3O^\bullet$ species generated in reactions 1–3 undergo further reactions to form stable organic compounds. The $CH_3O^\bullet$ undergoes rapid intermolecular hydrogen shift the form $^\bullet CH_2OH$ (*38*), or react with H donors to form methanol. $^\bullet CH_3$ can react with O_2, $^\bullet OH$ or other OH group donors to produce methanol. Under UV irradiation, methanol could be attacked by $^\bullet OH$ to form $^\bullet CH_2OH$ at the rate of $5 \times 10^8\ M^{-1}S^{1-}$ (Table S3, eq 1). $^\bullet CH_2OH$ could be oxidized directly by TiO_2 (Table S3, eq 3), and also could react with dissolved oxygen to form formaldehyde and superoxide ($HO_2^\bullet$) ($5 \times 10^9 M^{-1}S^{1-}$) (Table S3, eq 2). Formaldehyde can then be readily oxidized to formic acid at the rate of $1 \times 10^9 M^{-1}S^{1-}$ (Table S3, eq 4) so that it could not build up in solution. Although formic acid can be oxidized into CO_2 at the rate of $1.3 \times 10^8\ M^{-1}S^{1-}$ (reaction 5, Table S3), this mineralization reaction was not detected under these experimental conditions.

Supporting Information Available

Figure SI, control for the photocatalytical degradation of MMA and DMA; Table SI, photoreactions in the TiO_2 system; Table S2, quenching reactions of scavengers; Table S3, free radical reactions of methanol, formaldehyde, and formic acid. This material is available free of charge via the Internet at http://pubs.acs.org.

Literature Cited

(1) Anderson, L. C. D.; Bruland, K. D. Biogeochemistry of arsenic in natural waters: the importance of methylated species. *Environ. Sci. Technol.* **1991**, *25* (3), 420–429.

(2) Braman, R. S.; Foreback, C. C. Methylated forms of arsenic in the environment. *Science* **1973**, *182*, 1247–1249.

(3) Banerjee, K.; Helwick, R. P.; Gupta, S. A treatment process for removal of mixed inorganic and organic arsenic species from groundwater. *Environ. Prog.* **1999**, *18* (4), 280–284.

(4) Cullen, W. R.; Reimer, K. J. Arsenic speciation in the environment. *Chem. Rev.* **1989**, *89*, 713–764.

(5) Solo-Gabriele, H. ; Sakura-Lemessy, D.; Townsend, T.; Dubey, B.; Jambeck, J. *Quantities of Arsenic Within the State of Florida*; Florida Center for Solid and Hazardous Waste Management: Gainesville, FL, 2003.

(6) Pongratz, R. Arsenic speciation in environmental samples of contaminated soil. *Sci. Total Environ.* **1998**, *224*, 133–141.

(7) *Pesticides Industry Sales and Usage, 1998 and 1999 Market Estimates EPA*; U.S. Environmental Protection Agency: Washington, DC, 2002.

(8) Del Razo, L. M.; Arellano, M. A.; Cebrian, M. E. The oxidation states of arsenic in well water from a chronic arsenicism area of northern Mexico. *Environ. Pollut.* **1990**, *64*, 143–153.

(9) Chen, S. L.; Yeh, S. J.; Yang, M. H.; Lin, T. H. Trace element concentration and arsenic speciation in the well water of a Taiwan area with endemic blackfoot disease. *Biol. Trace Elem. Res.* **1995**, *48*, 263–274.

(10) Ghosh, M. M.; Yuan, J. R. Adsorption of inorganic arsenic and organoarsenicals on hydrous oxides. *Environ. Prog.* **1987**, *6* (3), 150–157.

(11) Vogels, C. M.; Johnson, M. D. *Arsenic Remediation in Drinking Waters Using Ferrate and Ferrous Ions*; New Mexico State University: Las Cruces, NM, 1998.

(12) Thirunavukkarasu, O. S.; Viraraghavan, T.; Subramanian, K. S.; Tanjore, S. Organic arsenic removal from drinking water. *Urban Water* **2002**, *4*, 415–421.

(13) Pena, M.; Meng, X.; Korfiatis, G. P.; Jing, C. Adsorption mechanism of arsenic on nanocrystalline titanium dioxide. *Environ. Sci. Technol.* **2006**, *40*, 1257–1262.

(14) Jing, C.; Meng, X.; Liu, S.; Baidas, S.; Patraju, R.; Christodoulatos, C.; Korfiatis, G. P. Surface complexation of organic arsenic on nanocrystalline titanium oxide. *J. Colloid Interface Sci.* **2005**, *290*, 14–21.

(15) Cullen, W. E.; Dodd, M. The photo-oxidation of solutions of arsenicals to arsenate: a convenient analytical procedure. *Appl. Organomet. Chem.* **1988**, *2*, 1–7.

(16) Nakajima, T.; Xu, Y. H.; Mori, Y.; Kishita, M.; Takanashi, H.; Maeda, S.; Ohki, A. Combined use of organoarsenic and adsorbent for the removal of inorganic arsenic and organoarsenic compounds from aqueous media. *J. Hazard. Mater.* **2005**, *B120*, 75–80.

(17) Xu, T.; Cai, Y.; O'Shea, K. Adsorption and photocatalyzed oxidation of methylated arsenic species in TiO2 suspensions. *Environ. Sci. Technol.* **2007**, *41*, 5471–5477.

(18) Hoffmann, M. R.; Martin, S. T.; Choi, W.; Bahnemann, D. W. Environmental applications of semiconductor photocatalysis. *Chem. Rev.* **1995**, *95*, 69–96.

(19) Bahnemann, D. W.; Hilgendorff, M.; Memming, R. Charge carrier dynamics at TiO2 particles: reactivity of free and trapped holes. *J. Phys. Chem. B*, **1997**, *101* (21), 4265–4275.

(20) Carp, O.; Huisman, C. L.; Reller, A. Photoinduced reactivity of titanium dioxide. *Prog. Solid State Chem.* **2004**, *32*, 33–177.

(21) Konaka, R.; kasahara, E.; Dunlap, W. C.; Yamamoto, Y.; Chien, K. C.; Inoue, M. Irradiation of titanium dioxide generates both singlet oxygen and superoxide anion. *Free Radical Biol. Med.* **1999**, *27* (Nos. 3/4), 294–300.

(22) Hoffmann, A. J.; Carraway, E. R.; Hoffmann, M. R. Photocatalytic production of H2O2 and organic peroxides on quantum-sized semiconductor colloids. *Environ. Sci. Technol.* **1994**, *28*, 776–785.

(23) Goto, H.; Hanada, Y.; Ohno, T.; Matsumura, M. Quantitative analysis of superoxide ion and hydrogen peroxide produced from molecular oxygen on photoirradiated TiO_2 particles. *J. Catal.* **2004**, *225*, 223–229.

(24) Daimon, T.; Nosaka, Y. Formation and behavior of singlet molecular oxygen in TiO_2 photocatalysis studied by detection of near-infrared phosphorescence. *J. Phys. Chem. C.* **2007**, *111* (11), 4420–4424.

(25) Meng, X. G.; Dadachov, M.; Korfiatis, G. P.; Christodoulatos, C. Method of preparing a surface-activated titanium oxide product and of using the same in water treatment processes. U.S. patent 6919029, 2005.

(26) Gomez-Ariza, J. L.; Sánchez-Rodas, D.; Beltran, R.; Corns, W.; Stockwel, P. Evaluation of atomic fluorescence spectrometry as a sensitive detection technique for arsenic speciation. *Appl. Organomet. Chem.* **1998**, *12*, 439–447.

(27) Sun, Y. C.; Chen, Y. J.; Tsai, Y. N. Determination of urinary arsenic species using an on-line nano-TiO2 photooxidation device coupled with microbore LC and hydride generation-ICP-MS system. *Microchem. J.* **2007**, *86*, 140–145.

(28) Xu, Y. H.; Nakajima, T.; Ohki, A. Adsorption and removal of arsenic (V) from drinking water by aluminum-loaded Shirasu-zeolite. *J. Hazard. Mater.* **2002**, *92* (3), 275–287.

(29) Yim, M. B.; Chock, P. B.; Stadtman, E. R. Copper, zinc superoxide dismutase catalyzes hydroxyl radical production from hydrogen peroxide. *Proc. Natl. Acad. Sci. USA.* **1990**, *87*, 5006–5010.

(30) Goldstone, A. B.; Liochev, S. I.; Fridovich, I. Inactivation of copper, zinc superoxide dismutase by H2O2: mechanism of protection. *Free Radical Biol. Med.* **2006**, *41*, 1860–1863.

(31) Buxton, G. V.; Greenstock, C. L.; Helman, W. P.; Ross, A. B. Critical review of rate constants for reactions of hydrated electrons. Hydrogen atoms and hydroxyl radicals (•OH/•O−) in aqueous solution. *J. Phys. Chem. Ref. Data* **1988**, *17*, 513–886.

(32) Ma, J.; Graham, N. J. D. Degradation of atrazine by manganese-catalysed ozonation-influence of radical scavengers. *Water Res.* **2000**, *34* (15), 3822–3828.

(33) Lanzalunga, O.; Bietti, M. Photo- and radiation chemical induced degradation of lignin model compounds. *J. Photochem. Photobiol., B* **2000**, *56*, 85–108.

(34) Steenken, S. Addition-elimination paths in electron-transfer reactions between radicals and molecules. Oxidation of organic molecules by the OH radical. *J. Chem. Soc., Faraday Trans. 1*, **1987**, *83*, 113–124.

(35) Oh, Y. C.; Bao, Y.; Jenks, W. S. Isotope studies of photocatalysis TiO2-mediated degradation of dimethyl phenylphosphonate. *J. Photochem. Photobiol., A* **2003**, *161*, 69–77.

(36) Aguila, A.; O'Shea, K. E.; Tobien, T.; Asmus, K. D. Reactions of hydroxyl radical with dimethyl methylphosphonate and diethyl methylphosphonate. A fundamental mechanistic study. *J. Phys. Chem. A* **2001**, *105* (33), 7834–7839.

(37) Macounová, K.; Krýsová, H.; Ludvík, J.; Jirkovský, J. Kinetics of photocatalytic degradation of diuron in aqueous colloidal solutions of Q-TiO_2 particles. *J. Photochem. Photobiol., A* **2003**, *156*, 273–282.

(38) Asmus, K. D.; Mockel, H.; Henglein, A. Pulse radiolytic study of the site of OH radical attack on aliphatic alcohols in aqueous solution. *J. Phys. Chem.* **1973**, *77*, 1218–1221.

ES0719677